Supplementary Information

Coordinating the interaction of ZnO and ZrO_2 for an efficient ethanol-to-butadiene process

Peng Wang[a], Shaowen Hou[a], Pengxiang Tu[a], Bing Xue[a], Weixin Guan[a], Dong Wang[a], Danfeng Zhou[a], Yajun He[a], Xinhui Chen[a], Yixing Wang[a], Kegong Fang[b], Xiaonian Li[a] and Jun Ni[a]*

[a] *State Key Laboratory of Green Chemistry Synthesis Technology, Institute of Industrial Catalysis, College of Chemical Engineering, Zhejiang University of Technology, Hangzhou, China*

[b] *State Key Laboratory of Coal Conversion, Institute of Coal Chemistry, Chinese Academy of Sciences, Taiyuan, China*

* Corresponding author and E-mail address: junni@zjut.edu.cn

Table of Contents

Table S1. Catalytic performance of catalysts reported in the literature.

Year	Catalyst	T (℃)	WHSV (h^{-1})	Conv. (%)	Sel. (%)	Yield (%)	Productivity ($g_{BD} \cdot g_{cat}^{-1} \cdot h^{-1}$)	Ref.
1950	2%Cr_2O_3-59%MgO–39%SiO_2	400	0.4	68	56	38	0.08	1
1985	SiO_2-MgO (1:1 mol%)	350	0.15	50	84	42	0.04	2
1988	Li^+-containing fluorohectorite	375	0.3	32	48	16	0.03	3
2012	3%Cr_2O_3-54%MgO-43%SiO_2	350	0.2	65	53	34	0.04	4
2012	3%ZnO-56%MgO-42%SiO_2	400	0.7	98	46	45	0.18	4
2012	3%CuO-56%MgO-42%SiO_2	400	0.7	86	53	44	0.18	4
2012	4%Ag-55%MgO-41%SiO_2	400	0.7	92	54	49	0.20	4
2015	1%Cu-1%Zr-0.5Zn%/SiO_2	360	0.21	96	65	63	0.08	5
2015	1%Cu-3%-Hf-0.5%Zn/SiO_2	360	0.21	99	72	71	0.09	5
2015	3%Hf-9.3%Zn/SiO_2	360	0.64	99	70	69	0.26	5
2015	ZnO/SiO_2-MgO	375	0.5	63	65	41	0.12	6
2016	$ZnZrO_x$	350	0.8	98	26	26	0.12	7
2016	Na-Zn-$Zr_{10}O_2$-H	350	0.2	97	47	46	0.05	7
2016	ZrZn/SiO_2-MgO	375	0.6	40	36	30	0.11	8
2016	SiO_2-MgO (sol-gel)	400	2.4	40	40	16	0.22	9
2017	Ga/SiO_2-MgO	400	0.08	99	53	52	0.02	10
2017	Cs_2O-ZnO-ZrO_2/SiO_2	400	1	98	56	55	0.32	11
2018	2%Cu/2%Zr-MTW	375	0.5	81	68	55	0.16	12
2018	t-ZrO_2+Cu/ZnO/Al_2O_3	400	2.9	76	54	42	0.72	13
2018	Zn-Talc	400	8.4	46	48	22	1.07	14
2018	6.1%Zn-3.4%Ta-TUD-1	400	8	82	63	52	2.44	15
2019	Cu-Ta/SiO_2	355	1.1	75	31	23	0.15	16
2019	3%Hf-9.3%Zn/SiO_2	360	1.12	87	43	38	0.25	17
2019	3%Hf-9.3%Zn/SiO_2	360	11.2	50	29	15	0.96	17
2019	ZnO/t-ZrO_2	375	2.8	94	47	44	0.72	18
2019	Hf-Zn/SiO_2	380	1.1	98	52	51	0.32	19
2020	ZnO-CeO_2/SBA-15	375	1.60	79	45	36	0.33	20
2020	ZnO/SiO_2-MgO	400	0.5	85	53	45	0.13	21
2020	ZnO-ZrO_2/SiO_2	400	5.0	67	59	39	1.14	22
2020	0.15Zn-0.225Y-DeAlBEA	400	12.24	94	52	49	3.52	23
2021	2%Zn-8%Y/beta	400	7.9	82	63	52	2.41	24
2021	ZnZrTUD-1	400	0.38	85	63	53	0.12	25
2022	10%SiO_2-ZrO_2	350	2.5	95	80	76	1.12	26
2022	Y-$Zn_{0.02}Zr_{0.02}$/Si-beta	350	1.0	80	60	48	0.28	27
2022	$Cu_1Zn_2Y_5$/SiBEA	375	1	99	70	69	0.41	28
2022	10%ZnCe@SBA-15	375	1.62	78	40	31	0.30	29
2022	ZnZr/SiO_2	400	0.77	92	61	56	0.25	30
2022	5%LaZnZr/Si-beta	350	1.0	83	61	51	0.30	31
2023	5Zn-3Zr/SBA-15	375	1.18	94	51	48	0.33	This

		375	12.0	36	55	20	1.39	work

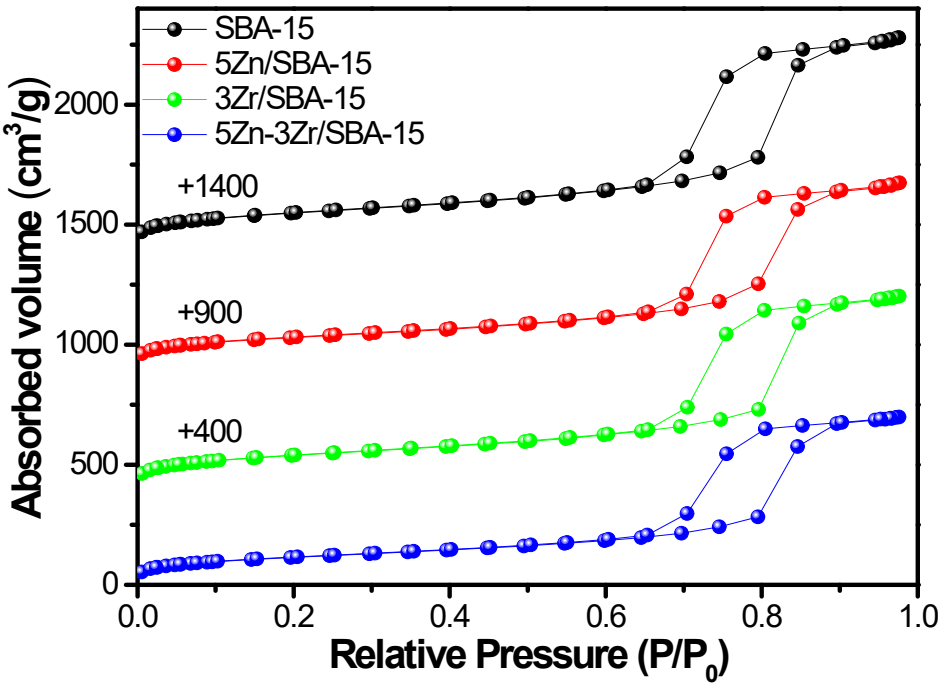

Figure S1. N_2 adsorption-desorption of the SBA-15 support and xZn-yZr/SBA-15 catalysts.

Table S2. Textural properties of the SBA-15 support and xZn-yZr/SBA-15 catalysts.

Catalyst	S_{BET}[a] (m^2/g)	V_t[b] (cm^3/g)	D_{pore}[c] (nm)
SBA-15	534.8	1.34	3.97
5Zn/SBA-15	468.0	1.12	3.97
3Zr/SBA-15	504.8	1.21	3.97
5Zn-3Zr/SBA-15	413.5	1.06	3.97

[a] BET surface area; [b] Single point pore volume at P/P_0=0.99; [c] Average pore diameter calculated by DFT method.

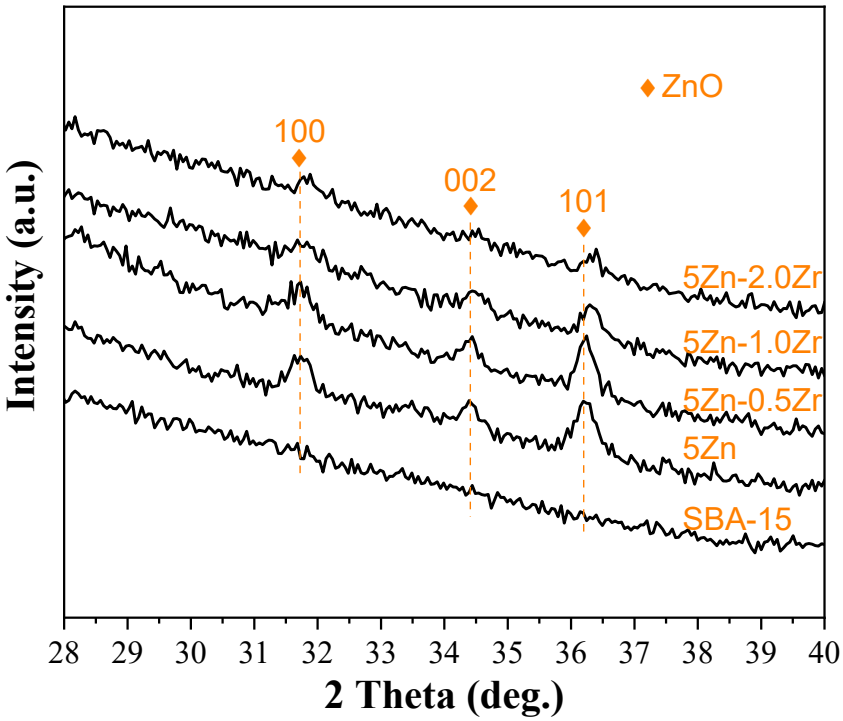

Figure S2. Zoom in of the region of 28-40° of Figure 1A.

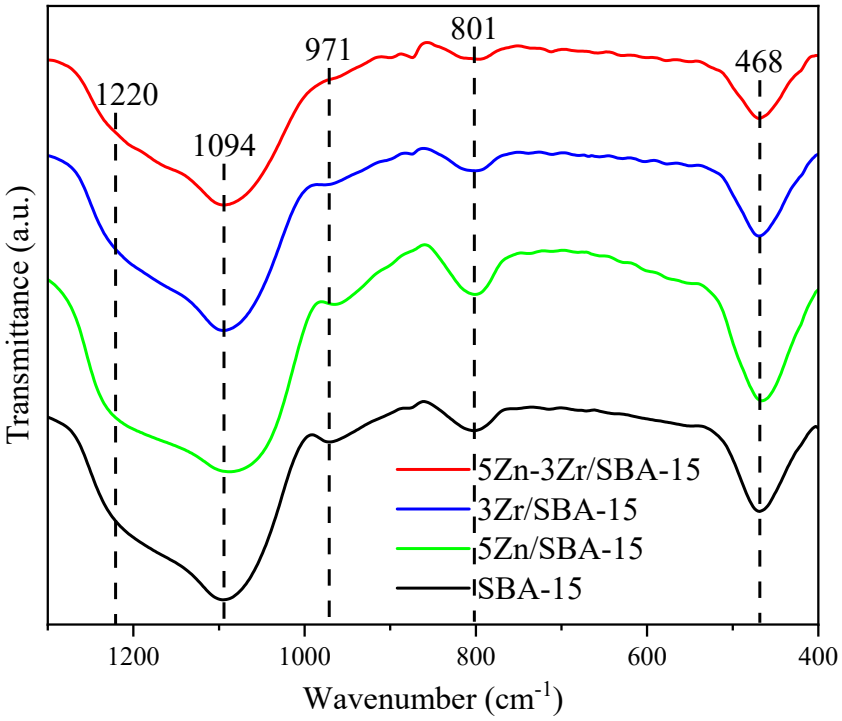

Figure S3. FTIR spectra of xZn-yZr/SBA-15 catalysts.

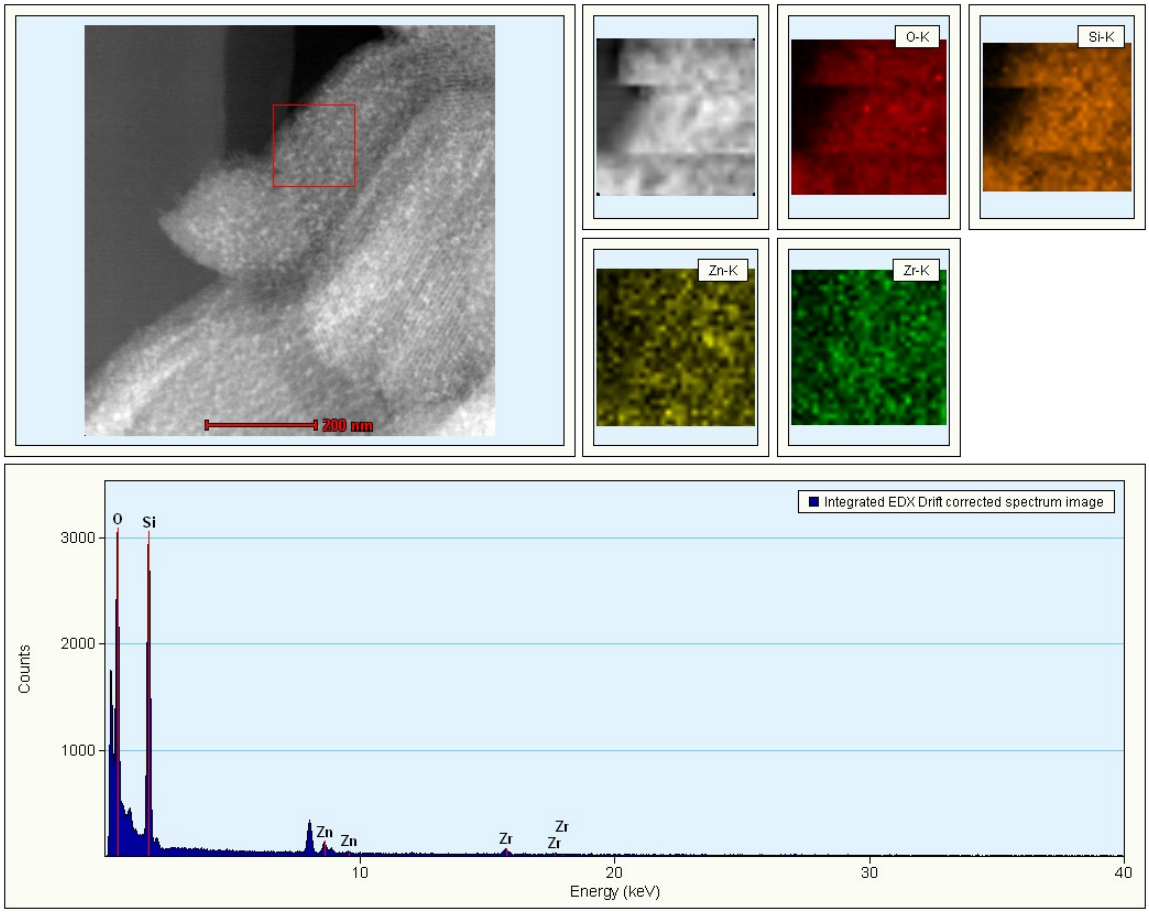

Figure S4. Element maps of 5Zn-3Zr/SBA-15 catalyst.

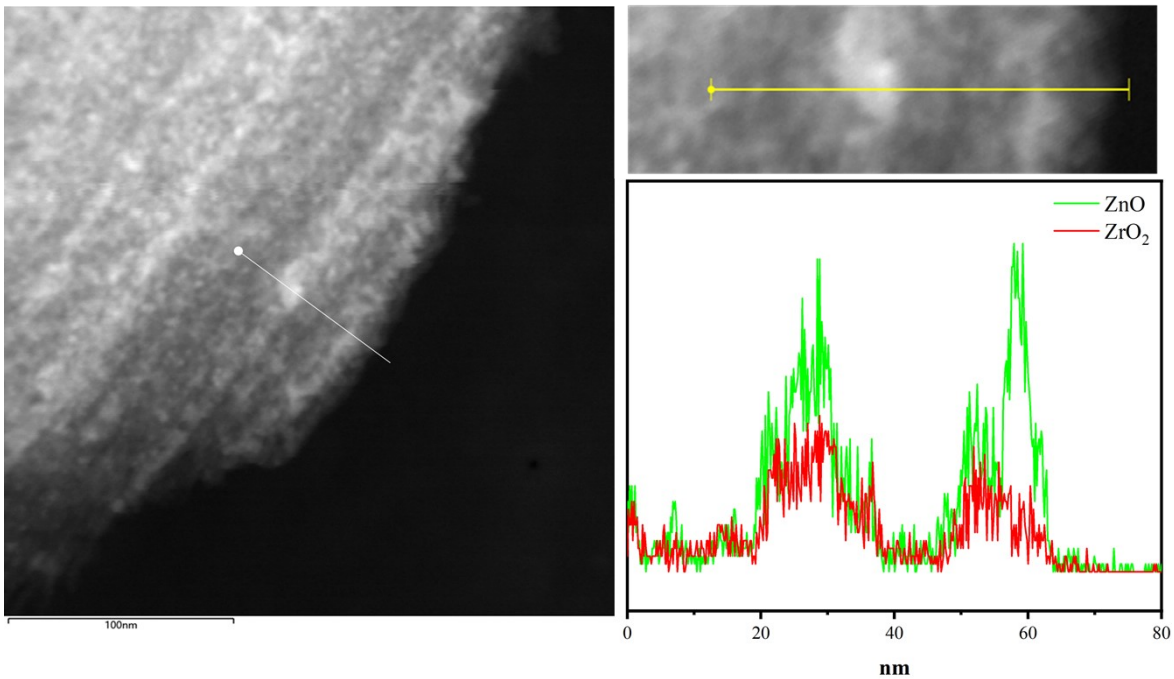

Figure S5. EDS line scan of 5Zn-3Zr/SBA-15 catalyst.

Table S3. Acid-base properties of xZn-yZr/SBA-15 catalysts with various contents of ZrO_2.

Catalyst	Acidic sites concentration[a] (mmol·g^{-1}), [T(ºC)][c]				Basic sites concentration[b] (mmol·g^{-1}), [T(ºC)][c]			
	SBA-15	Zn	Zr	Si-OH	SBA-15	Zn/Zr	Zn/Zr	Si-OH
5Zn	0.026	0.067		0.095	0.016	0.028	0.033	0.102
	[197]	[336]		[740]	[190]	[306]	[438]	[792]
5Zn-1Zr	0.016	0.041	0.005	0.069	0.016	0.038	0.027	0.093
	[185]	[327]	[491]	[747]	[198]	[332]	[470]	[786]
5Zn-2Zr	0.027	0.067	0.013	0.107	0.014	0.048	0.020	0.083
	[188]	[331]	[492]	[754]	[203]	[360]	[510]	[790]
5Zn-3Zr	0.025	0.074	0.019	0.117	0.015	0.048	0.016	0.087
	[200]	[338]	[508]	[771]	[210]	[367]	[510]	[776]
5Zn-4Zr	0.031	0.073	0.019	0.089	0.016	0.056	0.020	0.085
	[196]	[325]	[489]	[747]	[198]	[366]	[526]	[800]
5Zn-5Zr	0.036	0.074	0.030	0.144	0.016	0.059	0.024	0.075
	[195]	[327]	[495]	[762]	[196]	[371]	[545]	[800]

[a] Determined by NH_3-TPD; [b] Determined by CO_2-TPD; [c] The desorption temperature of TPD peaks.

Table S4. Acid-base properties of xZn-yZr/SBA-15 catalysts with various contents of ZnO.

Catalyst	Acidic sites concentration[a] (mmol·g^{-1}), [T(ºC)][c]				Basic sites concentration[b] (mmol·g^{-1}), [T(ºC)][c]			
	SBA-15	Zn	Zr	Si-OH	SBA-15	Zn/Zr	Zn/Zr	Si-OH
3Zr	0.048		0.063	0.101	0.023	0.078	0.023	0.175
	[208]		[457]	[776]	[228]	[390]	[550]	[760]
3Zn-3Zr	0.031	0.055	0.033	0.109	0.019	0.065	0.018	0.159
	[190]	[330]	[488]	[764]	[225]	[379]	[535]	[761]
4Zn-3Zr	0.021	0.057	0.010	0.156	0.015	0.054	0.013	0.113
	[194]	[332]	[493]	[771]	[208]	[371]	[514]	[766]
5Zn-3Zr	0.025	0.074	0.019	0.117	0.015	0.048	0.016	0.087
	[200]	[338]	[508]	[771]	[210]	[367]	[510]	[776]
6Zn-3Zr	0.028	0.073	0.025	0.129	0.015	0.048	0.018	0.168
	[199]	[337]	[500]	[782]	[212]	[365]	[506]	[761]
7Zn-3Zr	0.029	0.075	0.025	0.112	0.016	0.049	0.018	0.126
	[196]	[328]	[493]	[781]	[210]	[356]	[497]	[769]

[a] Determined by NH_3-TPD; [b] Determined by CO_2-TPD; [c] The desorption temperature of TPD peaks.

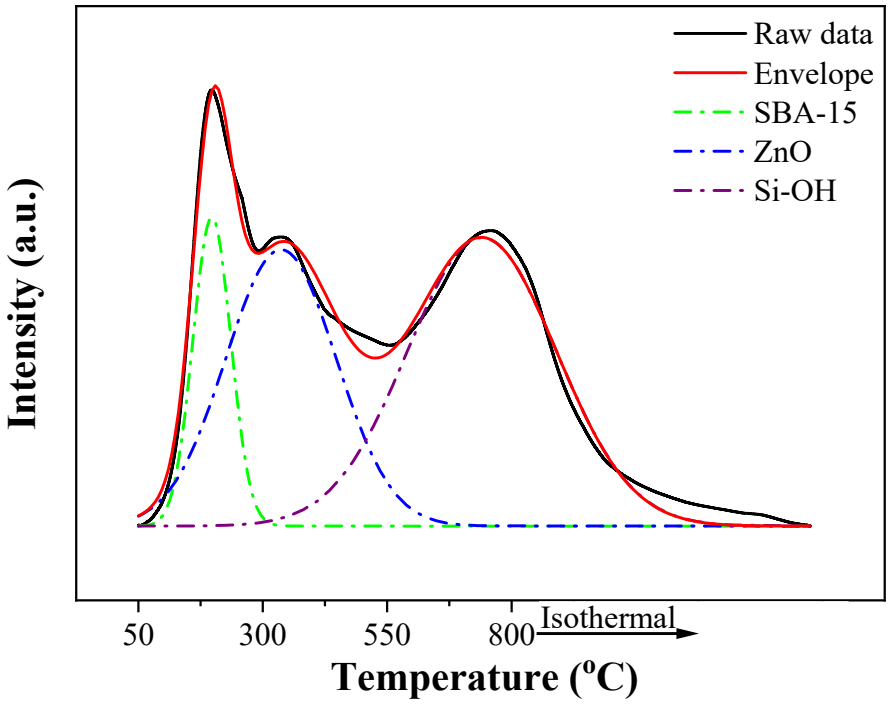

Figure S6. Deconvolution of NH_3-TPD profile of 5Zn/SBA-15 catalyst.

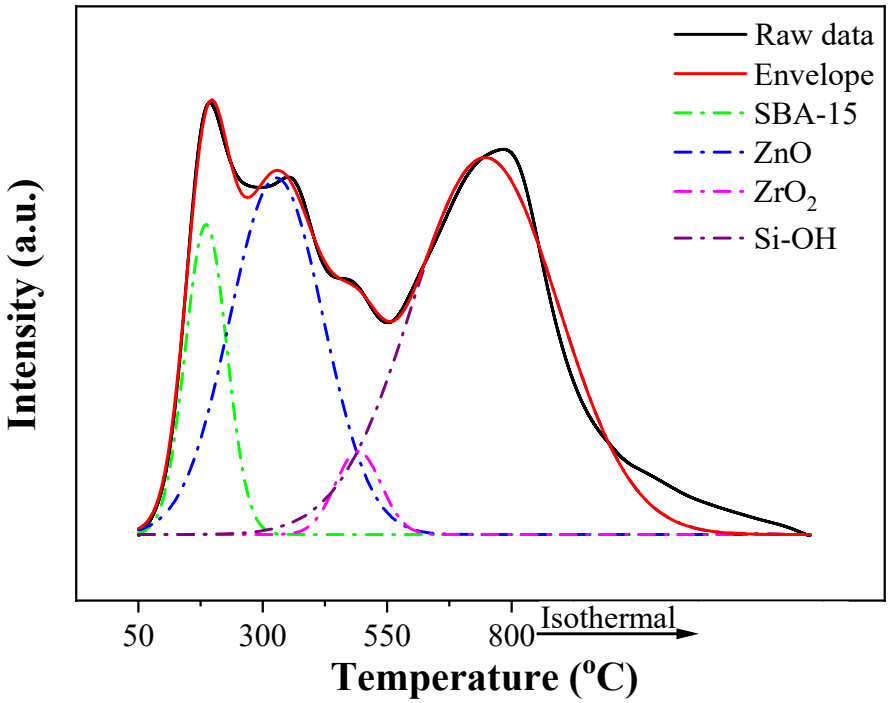

Figure S7. Deconvolution of NH_3-TPD profile of 5Zn-1Zr/SBA-15 catalyst.

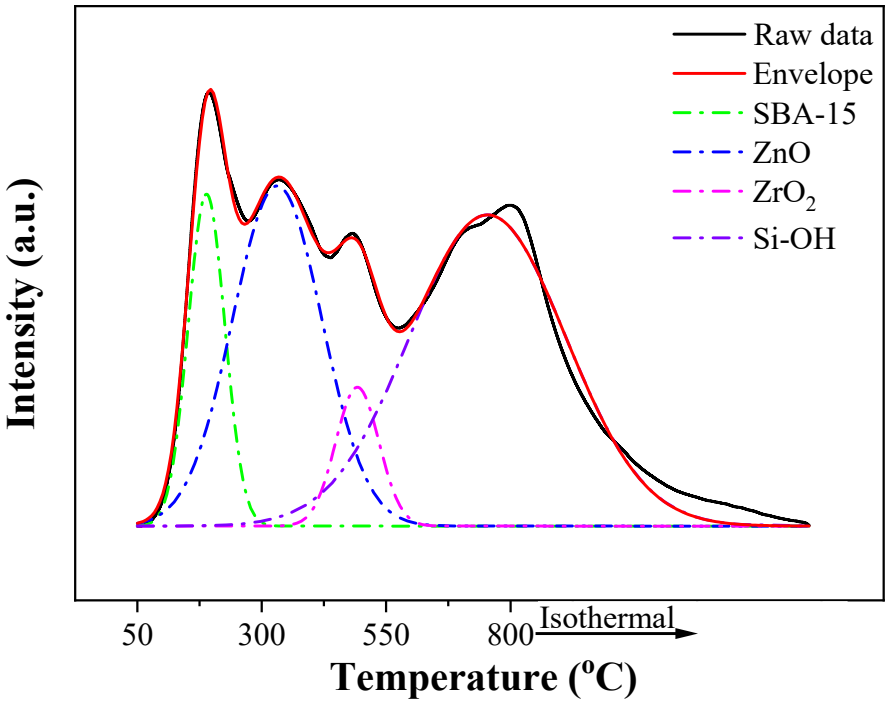

Figure S8. Deconvolution of NH_3-TPD profile of 5Zn-2Zr/SBA-15 catalyst.

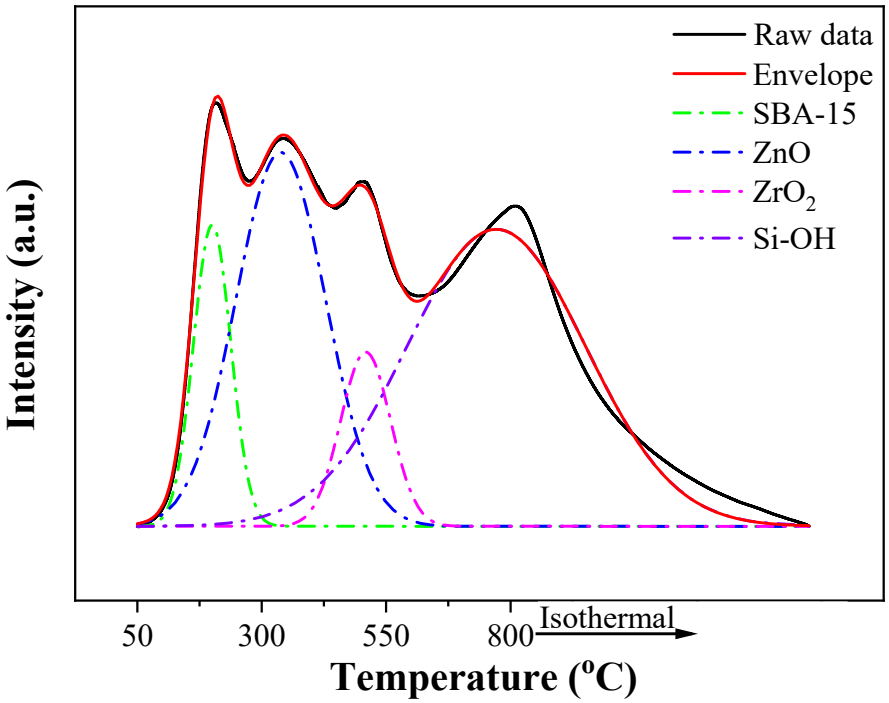

Figure S9. Deconvolution of NH_3-TPD profile of 5Zn-3Zr/SBA-15 catalyst.

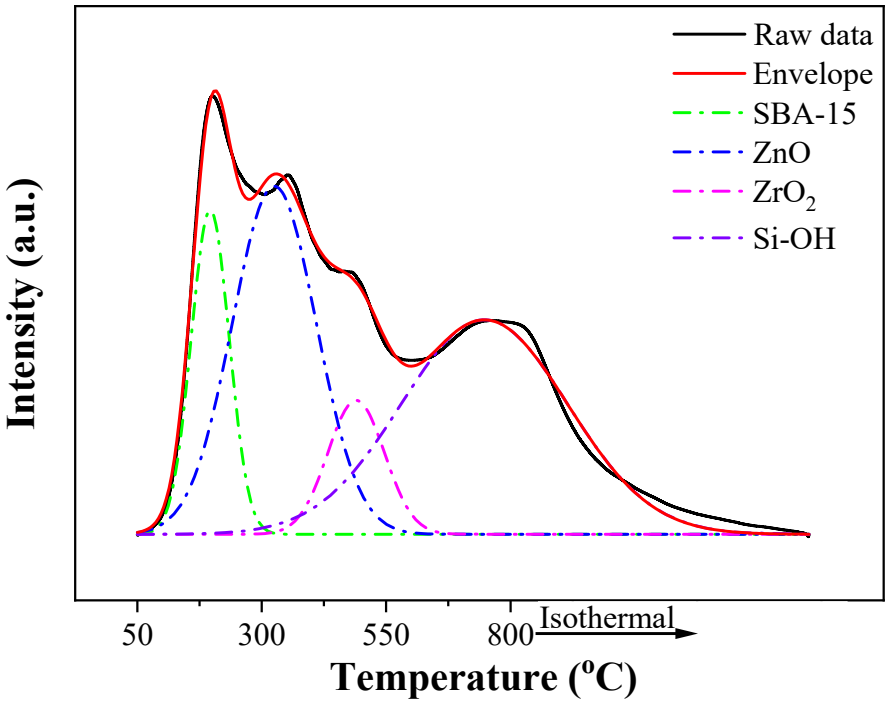

Figure S10. Deconvolution of NH_3-TPD profile of 5Zn-4Zr/SBA-15 catalyst.

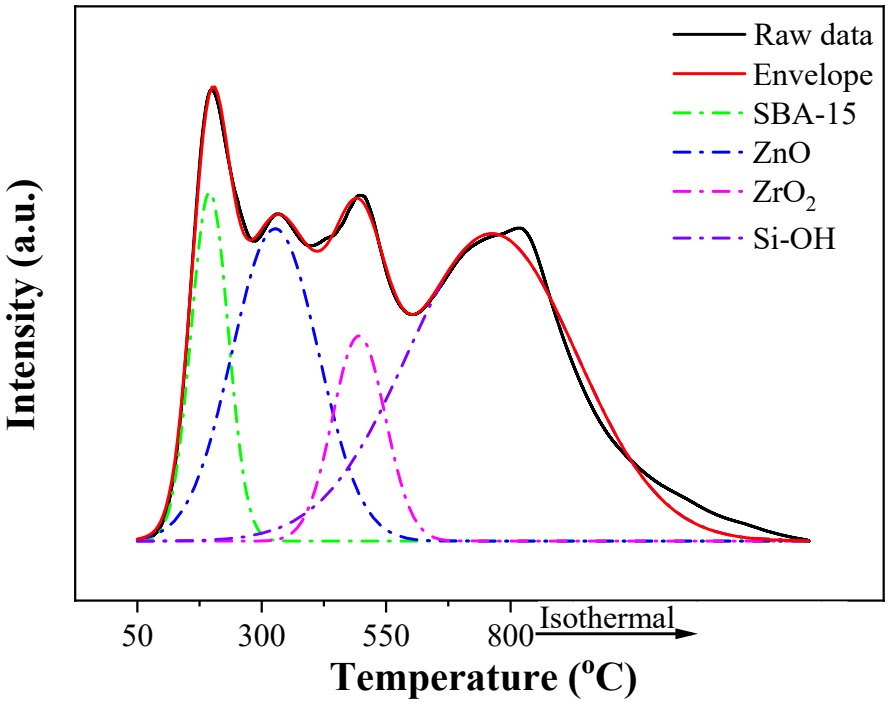

Figure S11. Deconvolution of NH_3-TPD profile of 5Zn-5Zr/SBA-15 catalyst.

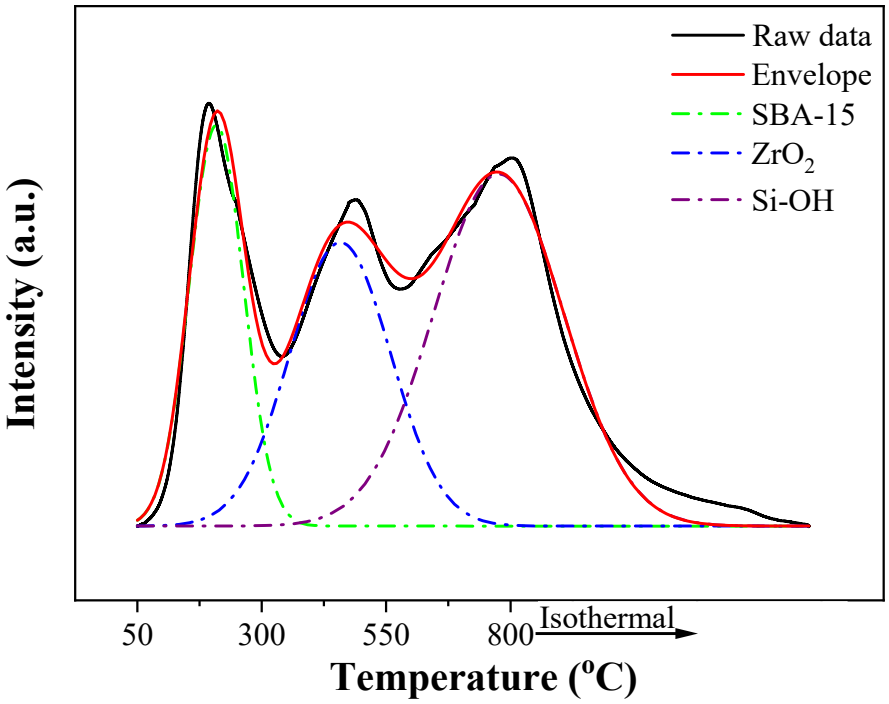

Figure S12. Deconvolution of NH_3-TPD profile of 3Zr/SBA-15 catalyst.

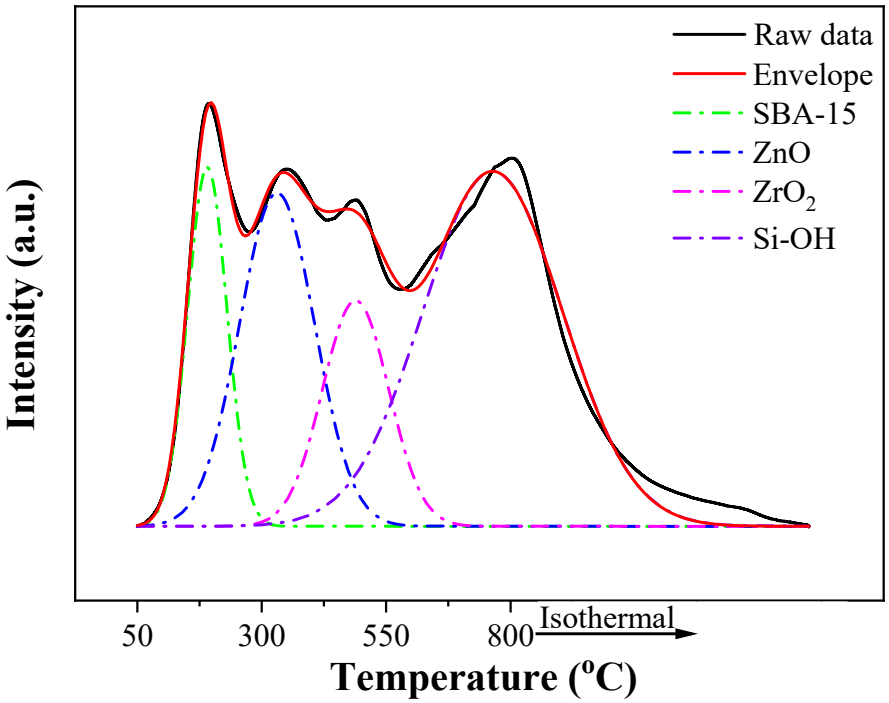

Figure S13. Deconvolution of NH_3-TPD profile of 3Zn-3Zr/SBA-15 catalyst.

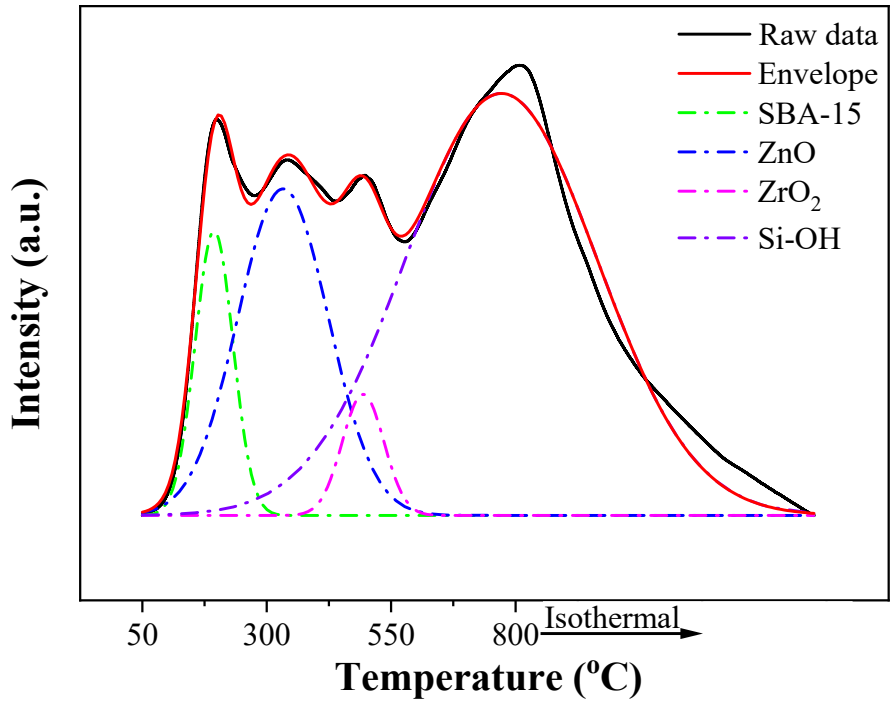

Figure S14. Deconvolution of NH_3-TPD profile of 4Zn-3Zr/SBA-15 catalyst.

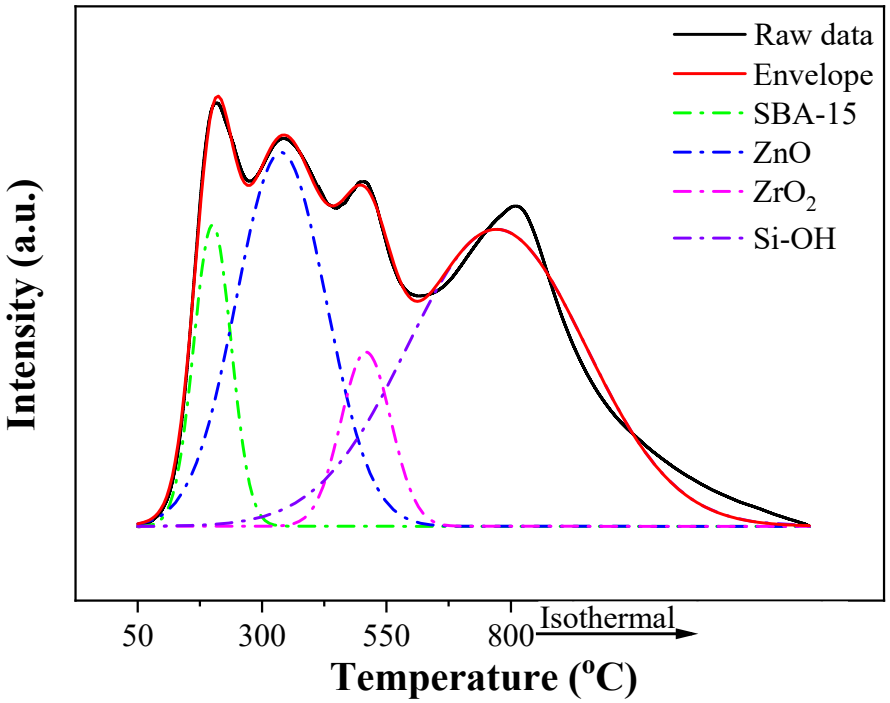

Figure S15. Deconvolution of NH_3-TPD profile of 5Zn-3Zr/SBA-15 catalyst.

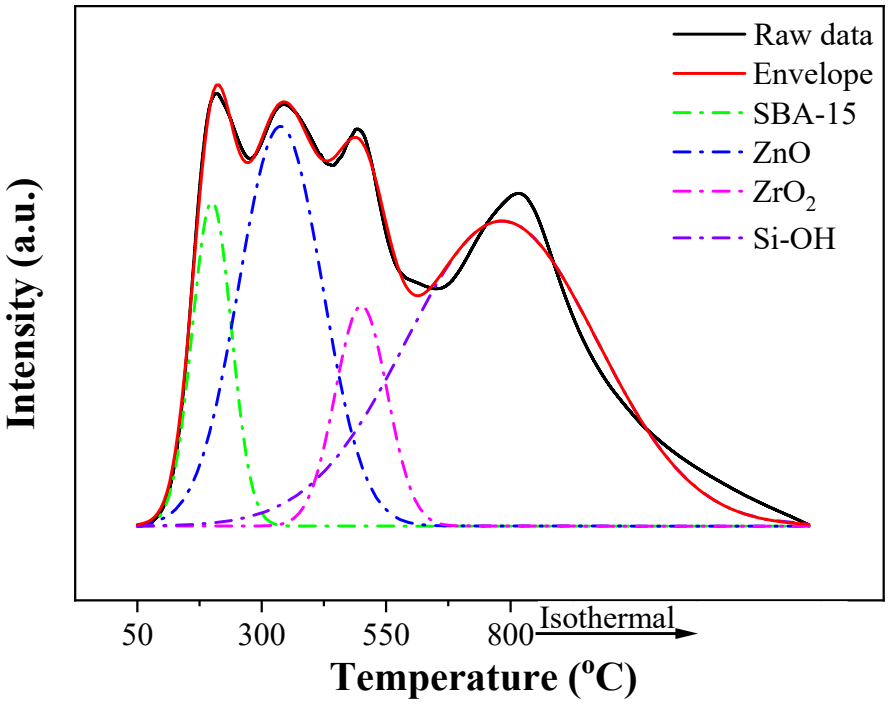

Figure S16. Deconvolution of NH_3-TPD profile of 6Zn-3Zr/SBA-15 catalyst.

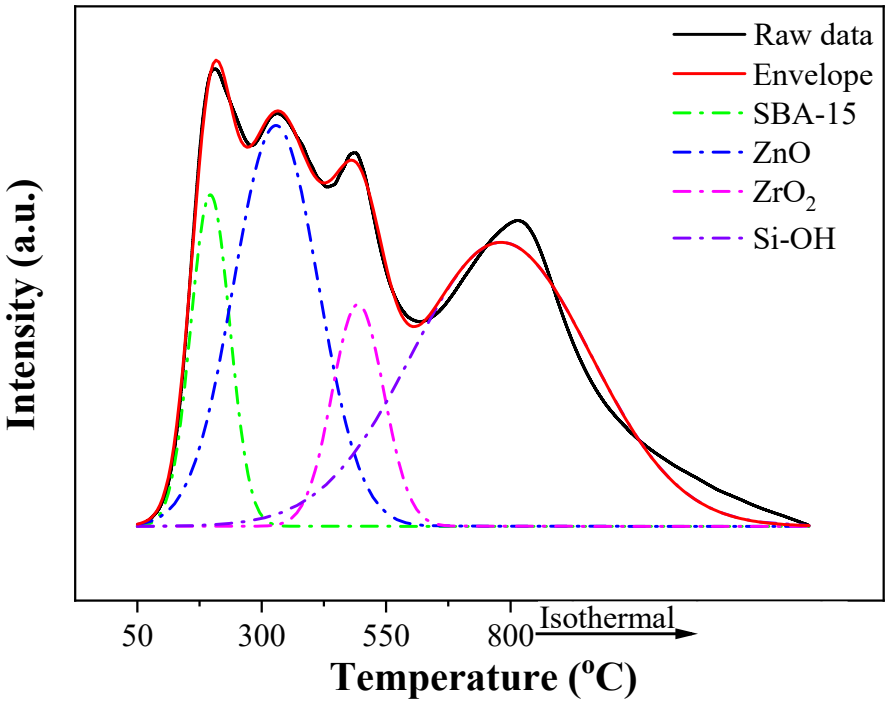

Figure S17. Deconvolution of NH_3-TPD profile of 7Zn-3Zr/SBA-15 catalyst.

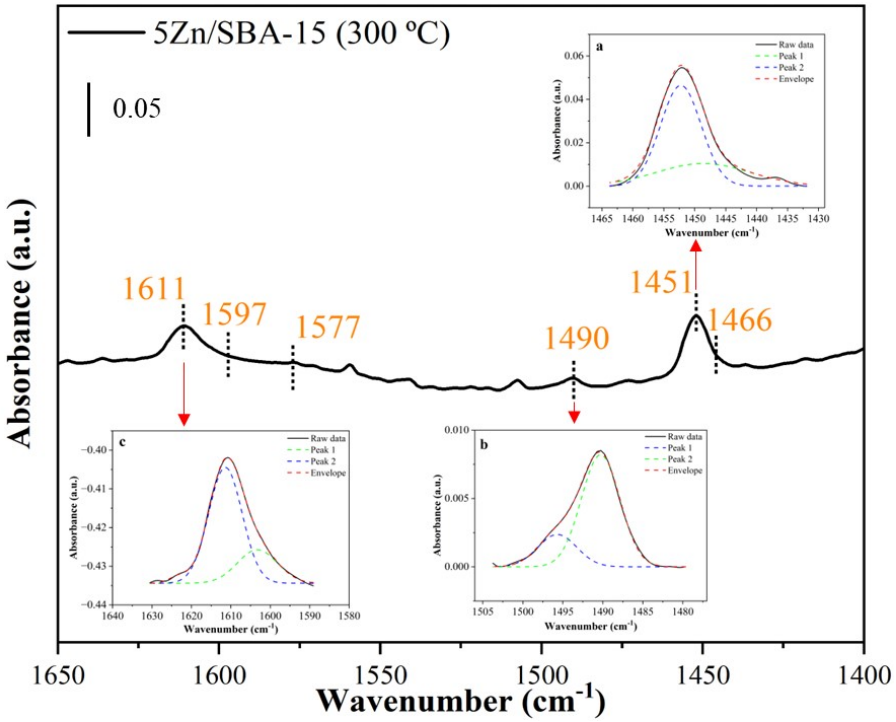

Figure S18. FTIR of pyridine adsorption and corresponding deconvolution over the 5Zn/SBA-15 catalyst at 300 ºC.

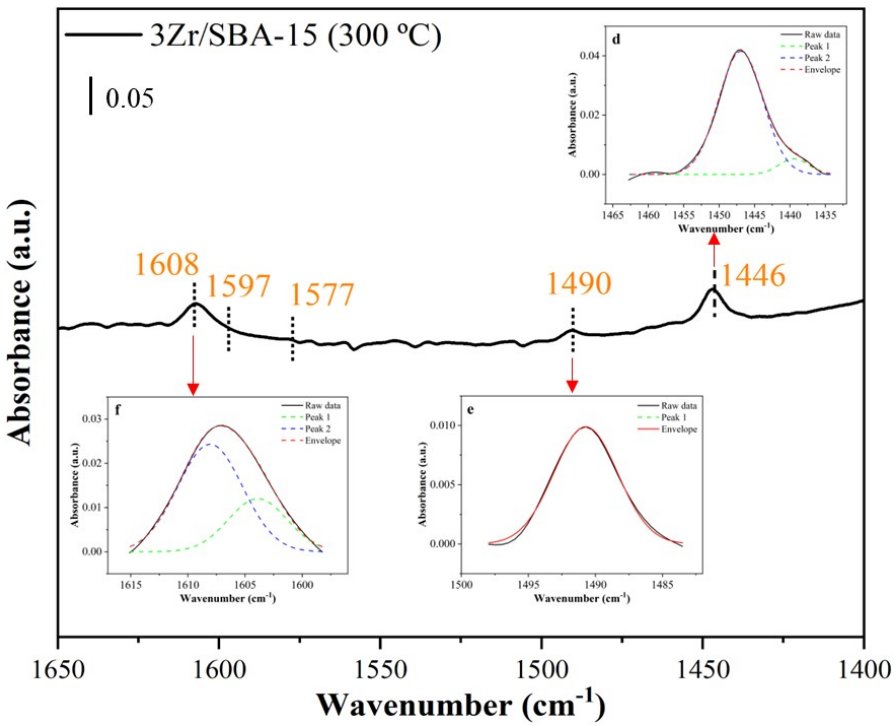

Figure S19. FTIR of pyridine adsorption and corresponding deconvolution over the 3Zr/SBA-15 catalyst at 300 ºC.

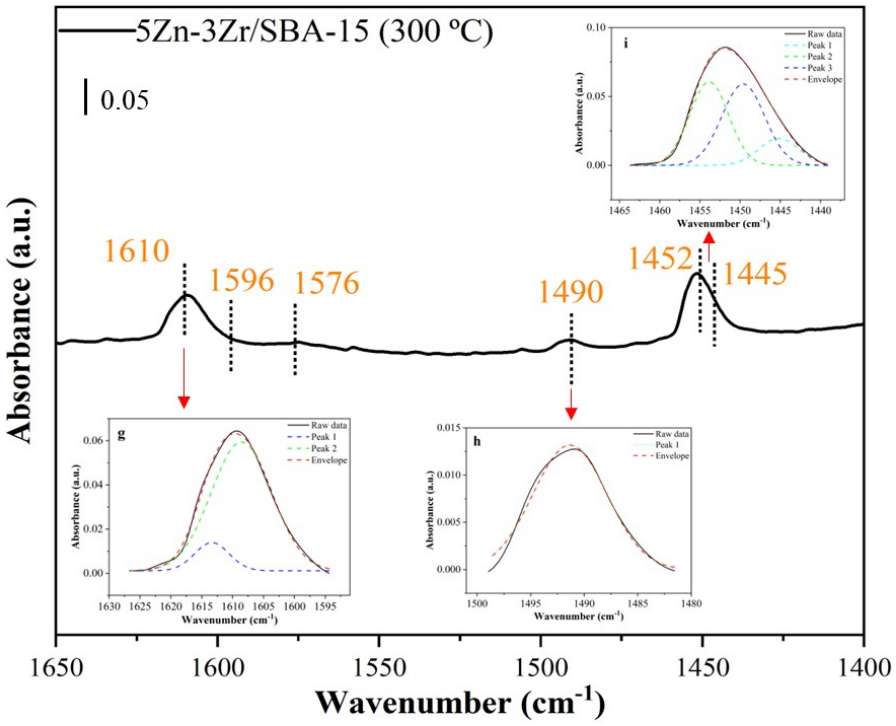

Figure S20. FTIR of pyridine adsorption and corresponding deconvolution over the 5Zn-3Zr/SBA-15 catalyst at 300 ºC.

Table S5. Deconvoluted band area under the characteristic bands of xZn-yZr/SBA-15 catalysts.

Catalyst	Band position (cm^{-1})				
	1611	1608	1490	1451	1446
5Zn/SBA-15	0.31827		0.4953	0.38231	
3Zr/SBA-15		0.17174	0.0589		0.35385
5Zn-3Zr/SBA-15	0.08936	0.71896	0.11231	0.39349	0.12029

There is a strong correlation between the deconvolution results and the NH_3-TPD results, as follows:

1. The band area at 1451 cm^{-1} for the 5Zn/SBA-15 catalyst (0.38231) is larger than that at 1446 cm^{-1} for the 3Zr/SBA-15 catalyst (0.35385), which aligns with the higher concentration of acidic sites in the 5Zn/SBA-15 catalyst (0.067 mmol g^{-1}) compared to 3Zr/SBA-15 (0.063 mmol g^{-1}).

2. The band area at 1451 cm^{-1} for the 5Zn-3Zr/SBA-15 catalyst (0.39349) exceeds that for the 5Zn/SBA-15 catalyst (0.38231), consistent with the higher concentration of Zn Lewis acid sites in the 5Zn-3Zr/SBA-15 catalyst (0.074 mmol g^{-1}) compared to 5Zn/SBA-15 (0.067 mmol g^{-1}).
3. The band area at 1446 cm^{-1} for the 5Zn-3Zr/SBA-15 catalyst is 0.12029, approximately one-third of that for the 3Zr/SBA-15 catalyst (0.35385), corresponding to the lower concentration of Zr Lewis acid sites in the 5Zn-3Zr/SBA-15 catalyst (0.019 mmol g^{-1}) compared to 3Zr/SBA-15 (0.063 mmol g^{-1}). This deviation from the nominal content suggests the deposition of ZnO onto ZrO_2.

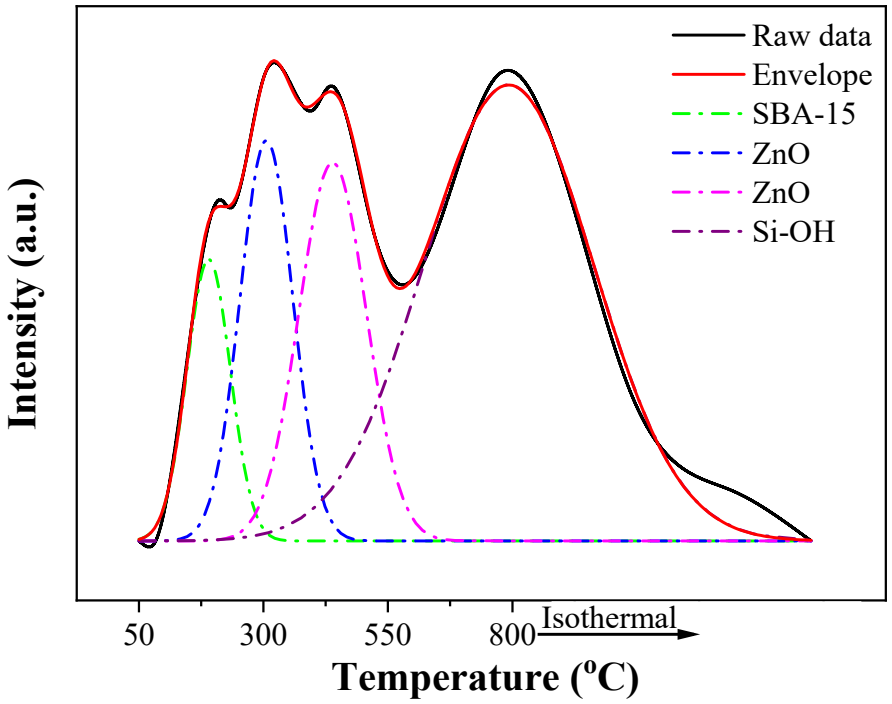

Figure S21. Deconvolution of CO_2-TPD profile of 5Zn/SBA-15 catalyst.

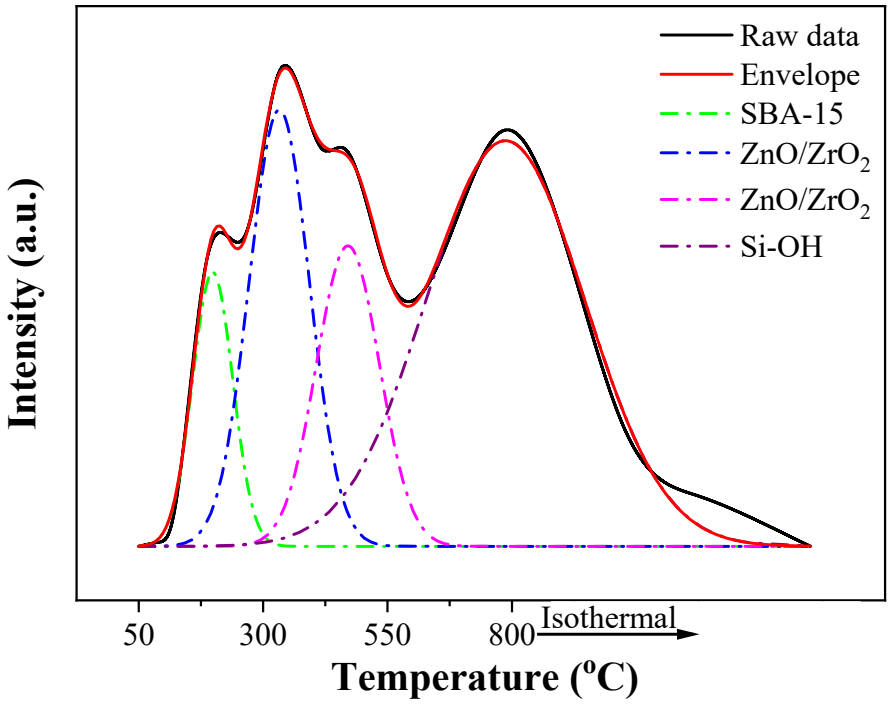

Figure S22. Deconvolution of CO_2-TPD profile of 5Zn-1Zr/SBA-15 catalyst.

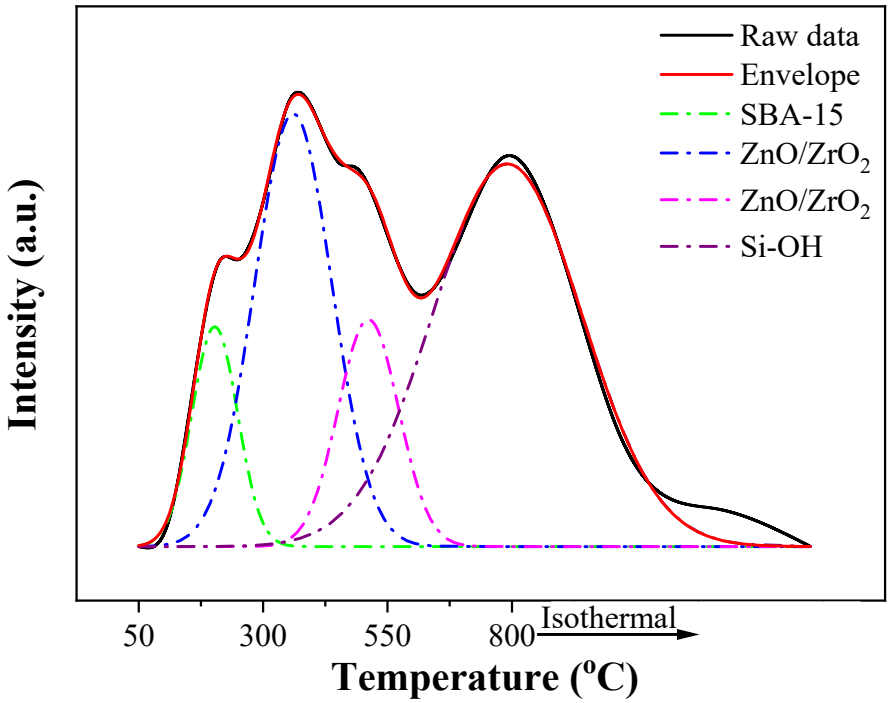

Figure S23. Deconvolution of CO_2-TPD profile of 5Zn-2Zr/SBA-15 catalyst.

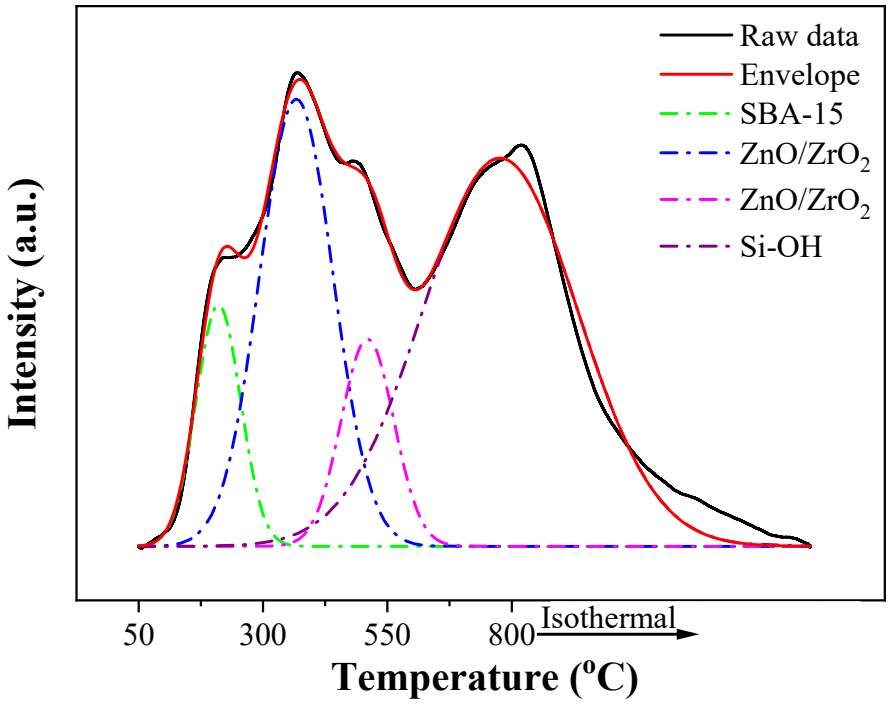

Figure S24. Deconvolution of CO_2-TPD profile of 5Zn-3Zr/SBA-15 catalyst.

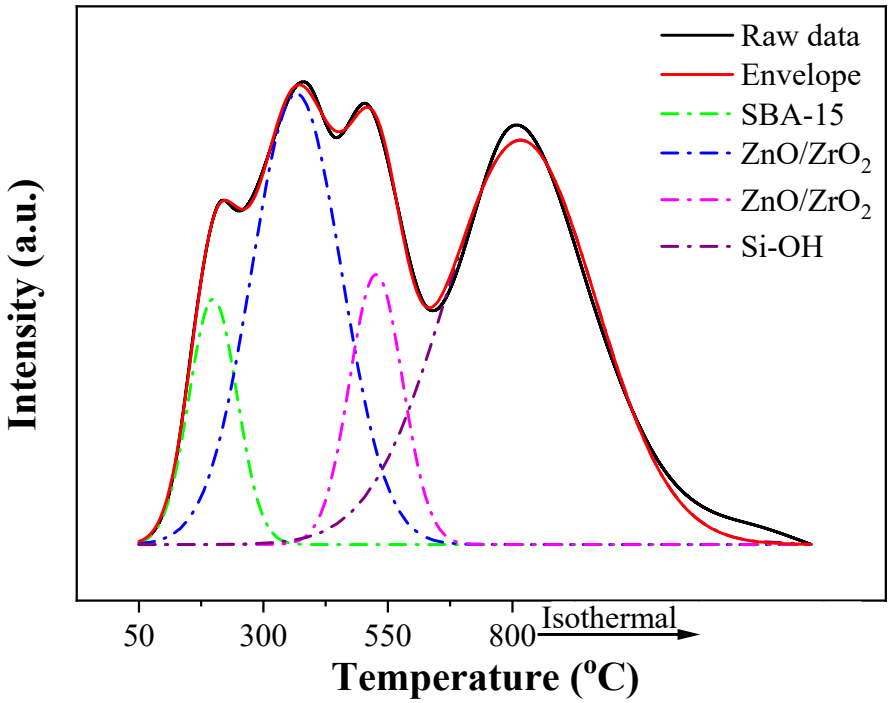

Figure S25. Deconvolution of CO_2-TPD profile of 5Zn-4Zr/SBA-15 catalyst.

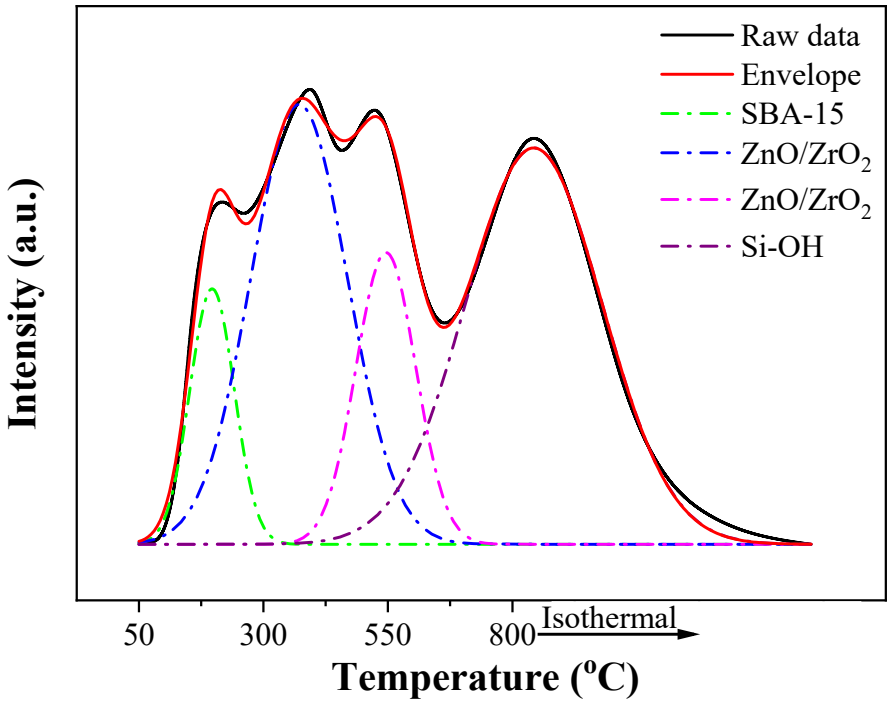

Figure S26. Deconvolution of CO_2-TPD profile of 5Zn-5Zr/SBA-15 catalyst.

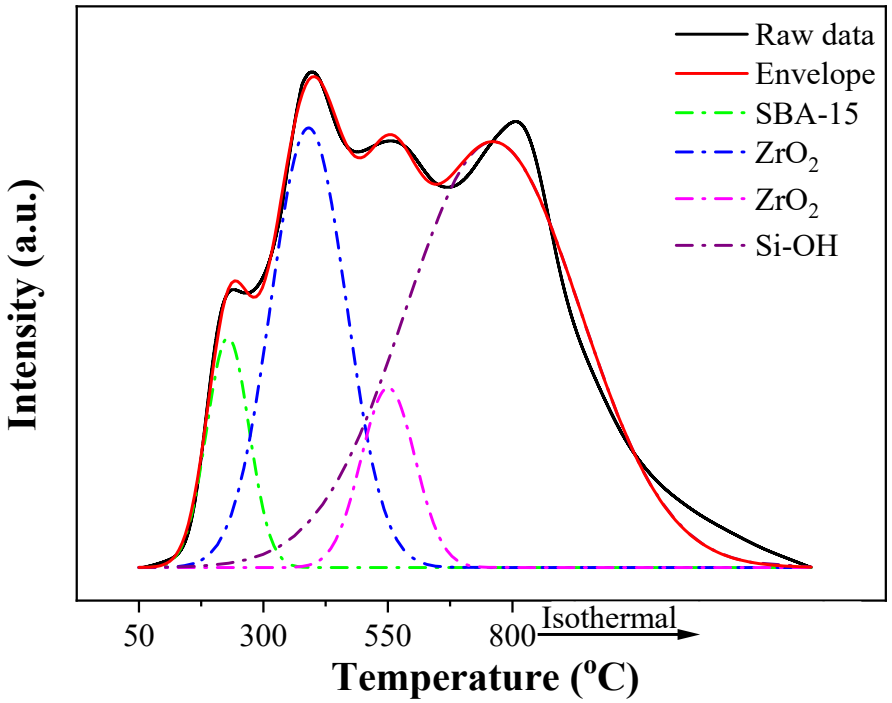

Figure S27. Deconvolution of CO_2-TPD profile of 3Zr/SBA-15 catalyst.

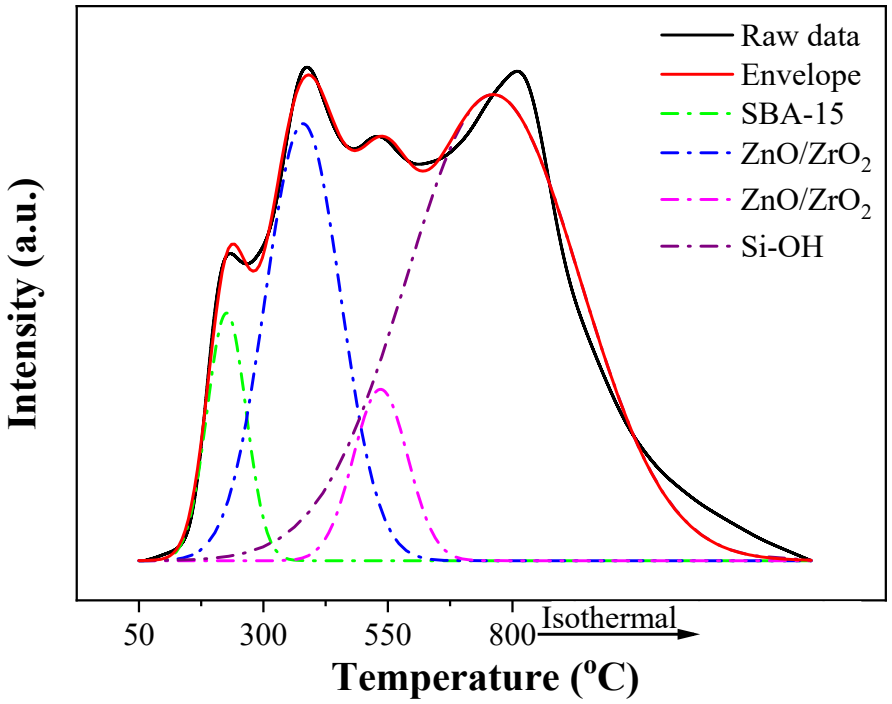

Figure S28. Deconvolution of CO_2-TPD profile of 3Zn-3Zr/SBA-15 catalyst.

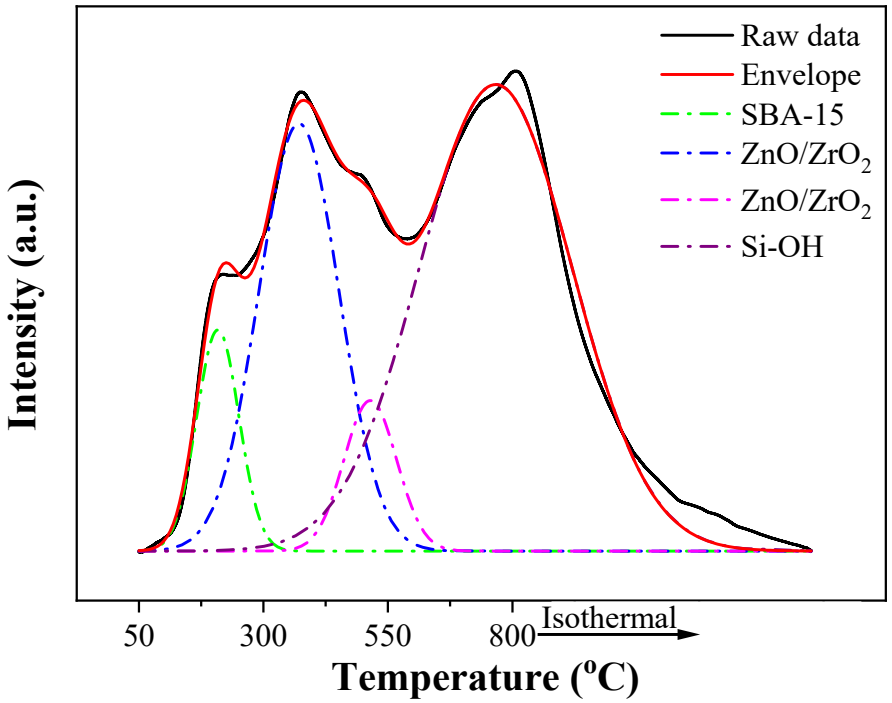

Figure S29. Deconvolution of CO_2-TPD profile of 4Zn-3Zr/SBA-15 catalyst.

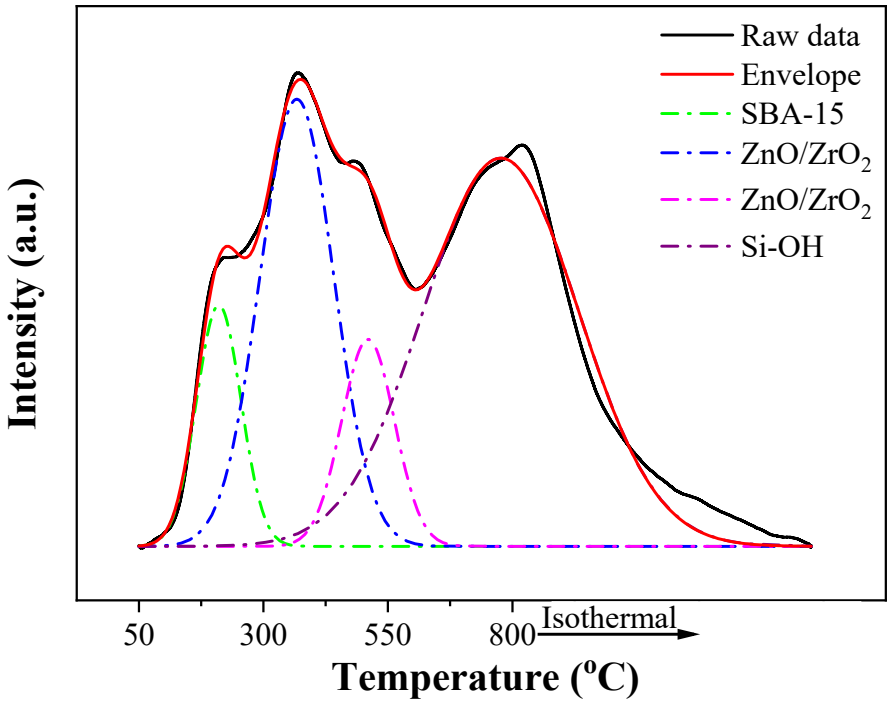

Figure S30. Deconvolution of CO_2-TPD profile of 5Zn-3Zr/SBA-15 catalyst.

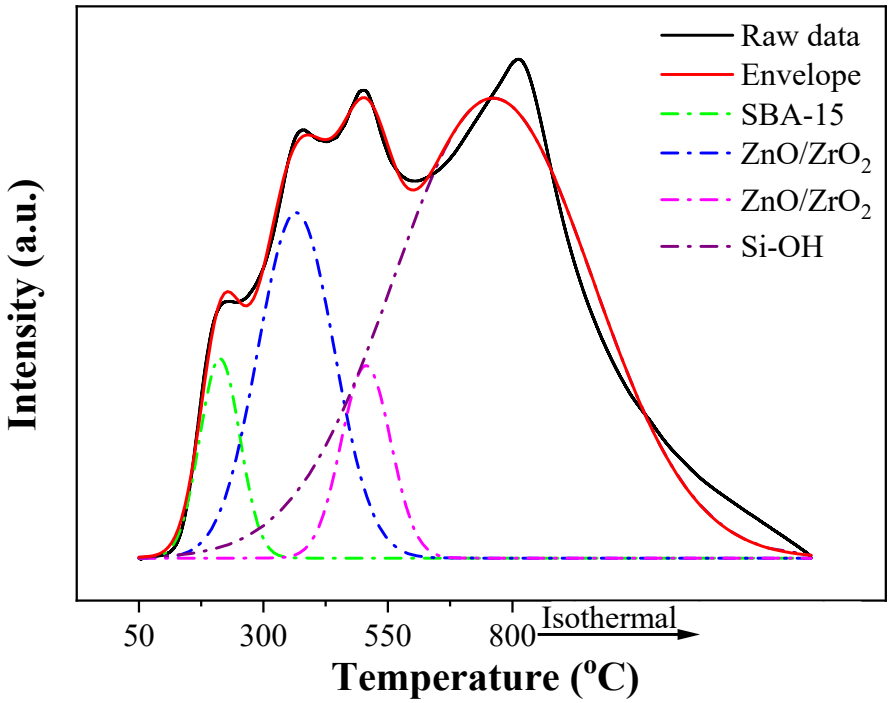

Figure S31. Deconvolution of CO_2-TPD profile of 6Zn-3Zr/SBA-15 catalyst.

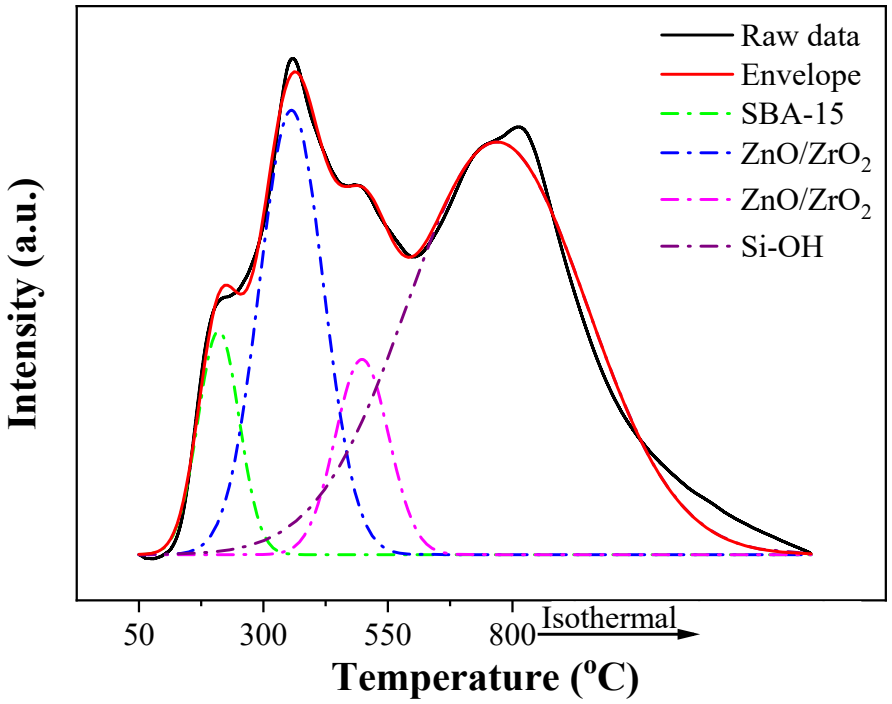

Figure S32. Deconvolution of CO_2-TPD profile of 7Zn-3Zr/SBA-15 catalyst.

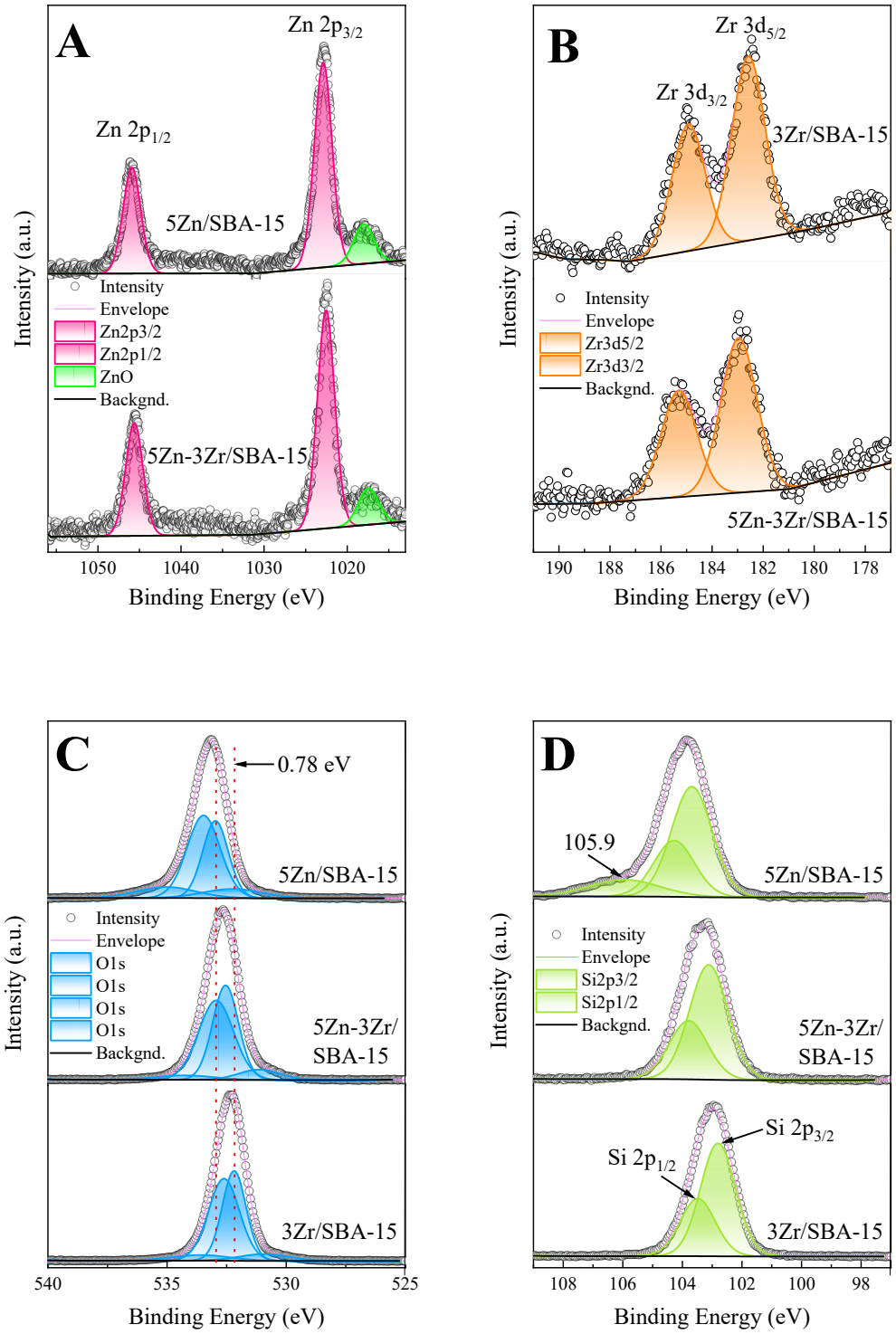

Figure S33. High-resolution XPS spectra of xZn-yZr/SBA-15 catalysts: (A) Zn 2p, (B) Zr 3d, (C) O 1s, and (D) Si 2p.

Table S6. Atomic content of constituent elements of xZn-yZr/SBA-15 catalysts.

Catalyst	Atomic %			
	Zn	Zr	Si	O
5Zn/SBA-15	0.57		31.05	59.97
3Zr/SBA-15		0.35	31.50	58.90
5Zn-3Zr/SBA-15	0.69	0.30	29.77	58.24

References

1. B. B. Corson, H. E. Jones, C. E. Welling, J. A. Hinckley and E. E. Stahly, *Ind. Eng. Chem.*, 1950, **42**, 359-373.
2. R. Ohnishi, T. Akimoto and K. Tanabe, *J. Chem. Soc., Chem. Commun.*, 1985, 1613-1614.
3. E. Suzuki, S. Idemura and Y. Ono, *Appl. Clay Sci.*, 1988, **3**, 123-134.
4. E. V. Makshina, W. Janssens, B. F. Sels and P. A. Jacobs, *Catal. Today*, 2012, **198**, 338-344.
5. T. De Baerdemaeker, M. Feyen, U. Müller, B. Yilmaz, F.-S. Xiao, W. Zhang, T. Yokoi, X. Bao, H. Gies and D. E. De Vos, *ACS Catal.*, 2015, **5**, 3393-3397.
6. O. V. Larina, P. I. Kyriienko and S. O. Soloviev, *Catal. Lett.*, 2015, **145**, 1162-1168.
7. R. A. L. Baylon, J. Sun and Y. Wang, *Catal. Today*, 2016, **259**, 446-452.
8. S. Da Ros, M. D. Jones, D. Mattia, J. C. Pinto, M. Schwaab, F. B. Noronha, S. A. Kondrat, T. C. Clarke and S. H. Taylor, *ChemCatChem*, 2016, **8**, 2376-2386.
9. J. V. Ochoa, C. Bandinelli, O. Vozniuk, A. Chieregato, A. Malmusi, C. Recchi and F. Cavani, *Green Chem.*, 2016, **18**, 1653-1663.
10. J. V. Ochoa, A. Malmusi, C. Recchi and F. Cavani, *ChemCatChem*, 2017, **9**, 2128-2135.
11. P. T. Patil, D. Liu, Y. Liu, J. Chang and A. Borgna, *Appl. Catal. A-Gen.*, 2017, **543**, 67-74.
12. M. M. Kurmach, O. V. Larina, P. I. Kyriienko, P. S. Yaremov, V. V. Trachevsky, O. V. Shvets and S. O. Soloviev, *ChemistrySelect*, 2018, **3**, 8539-8546.
13. L. H. Chagas, C. R. V. Matheus, P. C. Zonetti and L. G. Appel, *Molecular Catalysis*, 2018, **458**, 272-279.
14. A. Miyaji, M. Hiza, Y. Sekiguchi, S. Akiyama, A. Shiga and T. Baba, *J. Jpn. Pet. Inst.*, 2018, **61**, 171-181.
15. G. Pomalaza, G. Vofo, M. Capron and F. Dumeignil, *Green Chem.*, 2018, **20**, 3203-3209.
16. D. D. Dochain, A. Stýskalík and D. P. Debecker, *Catalysts*, 2019, **9**, 920.
17. G. M. Cabello González, R. Murciano, A. L. Villanueva Perales, A. Martínez, F. Vidal-Barrero and M. Campoy, *Appl. Catal. A-Gen.*, 2019, **570**, 96-106.
18. L. H. Chagas, P. C. Zonetti, C. R. V. Matheus, C. R. K. Rabello, O. C. Alves and L. G. Appel, *ChemCatChem*, 2019, **11**, 5625-5632.
19. G. M. Cabello González, P. Concepción, A. L. Villanueva Perales, A. Martínez, M. Campoy and F. Vidal-Barrero, *Fuel Process. Technol.*, 2019, **193**, 263-272.
20. Y. Zhao, S. Li, Z. Wang, S. Wang, S. Wang and X. Ma, *Chin. Chem. Lett.*, 2020, **31**, 535-538.
21. B. Szabó, G. Novodárszki, Z. Pászti, A. Domján, J. Valyon, J. Hancsók and R. Barthos, *ChemCatChem*, 2020, **12**, 5686-5696.
22. T. Miyazawa, Y. Tanabe, I. Nakamura, Y. Shinke, M. Hiza, Y.-K. Choe and T. Fujitani, *Catal. Sci. Technol.*, 2020, **10**, 7531-7541.
23. L. Qi, Y. Zhang, M. A. Conrad, C. K. Russell, J. Miller and A. T. Bell, *J. Am. Chem. Soc.*, 2020, **142**, 14674-

14687.
24. W. Dai, S. Zhang, Z. Yu, T. Yan, G. Wu, N. Guan and L. Li, *ACS Catal.*, 2017, **7**, 3703-3706.
25. K. Wang, L. Guo, W. Gao, B. Zhang, H. Zhao, J. Liang, N. Liu, Y. He, P. Zhang, G. Yang and N. Tsubaki, *ACS Sustain. Chem. Eng.*, 2021, **9**, 10569-10578.
26. A. A. Bojang and H.-S. Wu, *Catalysts*, 2022, **12**, 766.
27. K. Wang, X. Peng, C. Wang, W. Gao, N. Liu, X. Guo, Y. He, G. Yang, L. Jiang and N. Tsubaki, *Catal. Sci. Technol.*, 2022, **12**, 2210-2222.
28. H. Dai, T. Ye, K. Wang, M. Zhang, L.-M. Wu and G. Ouyang, *Catalysts*, 2022, **12**, 1147.
29. Z. Wang, S. Li, S. Wang, J. Liu, Y. Zhao and X. Ma, *Chin. J. Chem. Eng.*, 2022, **45**, 162-170.
30. N. Liu, L. Zhang, K. Wang, L. Shao, X. Guo, Y. He, Z. Wu, P. Zhan, G. Liu, J. Wu, G. Yang and N. Tsubaki, *Appl. Surf. Sci.*, 2022, **602**, 154299.
31. K. Wang, N. Liu, Q. Ma, Y. Kawabata, F. Wang, W. Gao, B. Zhang, X. Guo, Y. He, G. Yang and N. Tsubaki, *Catal. Today*, 2023, **411-412**, 113800.